Cancer Immunol Immunother (2017) 66:181–192
DOI 10.1007/s00262-016-1928-0

ORIGINAL ARTICLE

Immunogenicity and efficacy of a rationally designed vaccine against vascular endothelial growth factor in mouse solid tumor models

Aizhang Xu[1,2] · Li Zhang[1,2] · Yangyang Chen[1,2] · Zhibing Lin[1,2] · Rongxiu Li[1,2,3]

Received: 13 March 2016 / Accepted: 7 November 2016 / Published online: 21 November 2016

Abstract Vascular endothelial growth factor (VEGF) plays an important role in the progression of various cancers. The VEGF-specific antibody bevacizumab combined with chemotherapy was shown to significantly improve progression-free survival in certain cancers. However, repeated administration is necessary for effective suppression of VEGF, thereby making the therapy expensive and cumbersome. Thus, it is urgent to develop alternative reagents such as VEGF vaccines. Here we report that DTT-VEGF, a VEGF-based antigen consisting of the receptor-binding domain of VEGF and diphtheria toxin T domain (DTT), not only stimulated neutralizing antibody response, but also induced type 1 immune response as well as anti-tumor cytotoxic T lymphocytes in mice when administered with aluminum hydroxide adjuvant. The antibodies triggered by DTT-VEGF immunization inhibited the binding of VEGF to VEGF receptor and downregulated the serum VEGF levels in tumor-bearing mice. VEGF-specific IgG2a and IgG2b antibodies as well as type 1 cytokines were stimulated by DTT-VEGF vaccination. The splenocytes from DTT-VEGF-immunized mice showed cytotoxic activity against B16-F10 cells expressing VEGF. Extensive necrosis with severe hemorrhage and enhanced $CD8^+$ T cell infiltration were observed in tumors from DTT-VEGF-immunized mice. The percentages of $CD31^+$ vascular areas in the tumor sections from DTT-VEGF-immunized mice were significantly lower than those of control mice. DTT-VEGF significantly inhibited tumor growth in preventive and therapeutic vaccination settings in mouse models. Our data suggest that DTT is an effective antigen carrier to break immune self-tolerance and our vaccine design has potential to be used for human cancer therapy.

Keywords Cancer vaccine · Cytotoxic T lymphocytes · Diphtheria toxin T domain · Immunotherapy · Type 1 immune response · Vascular endothelial growth factor

Abbreviations

Alum	Aluminum hydroxide
CFSE	Carboxyfluorescein succinimidyl ester
CTLs	Cytotoxic T lymphocytes
DCs	Dendritic cells
DTT	Diphtheria toxin T domain
GST	Glutathione *S*-transferase
H&E	Hematoxylin and eosin
IFA	Incomplete Freund's adjuvant
LDH	Lactate dehydrogenase
mAbs	Monoclonal antibodies
SEM	Standard error of mean
VEGF	Vascular endothelial growth factor
VEGFR	Vascular endothelial growth factor receptor

Electronic supplementary material The online version of this article (doi:10.1007/s00262-016-1928-0) contains supplementary material, which is available to authorized users.

✉ Rongxiu Li
rxli@sjtu.edu.cn

[1] State Key Laboratory of Microbial Metabolism, Shanghai Jiao Tong University, 800 Dongchuan Road, Shanghai 200240, China

[2] School of Life Sciences and Biotechnology, Shanghai Jiao Tong University, Shanghai, China

[3] Engineering Research Center of Cell and Therapeutic Antibody, Ministry of Education, Shanghai Jiao Tong University, Shanghai, China

Introduction

Vascular endothelial growth factor (VEGF) secreted by tumor cells is the dominant growth factor promoting tumor neo-angiogenesis, a critical process in tumor progression and metastasis [1]. VEGF induces the formation of new blood vessels by stimulating endothelial cells in the normal vasculature to sprout into tumor. Moreover, high levels of VEGF in tumor-bearing hosts help cancer cells to evade immunological destruction by inhibiting the functions of dendritic cells (DCs) [2] and T cells [3], promoting the proliferation of regulatory T cells [4] and suppressing the infiltration of leukocytes into tumor tissues [5]. Therefore, stimulating an immune response against VEGF would have the potential to combine the benefits of anti-angiogenesis and immunotherapy.

Various regents have been tested to inhibit the function of VEGF [1], such as small molecular inhibitors of VEGF receptor (VEGFR) tyrosine kinase, soluble VEGFR, monoclonal antibodies (mAbs) against VEGF or its receptors. Particularly, anti-VEGF mAb bevacizumab combined with chemotherapy has shown clinical benefits in patients with metastatic breast cancer [6], non-small cell lung cancer [7] and metastatic colorectal cancer [8]. However, passive immunization with mAbs has several disadvantages. Repeated administration of large volume of antibody is necessary for effective suppression of VEGF as the antibodies are rapidly cleared from the circulation. MAbs often show immunogenicity themselves, thereby limiting their long-term use. Once the administration of mAbs discontinued, it may lead to relapse and regrowth of tumor, which is often associated with more invasive phenotype [9]. Consequently, it has little benefits on the overall survival. To circumvent these limitations, it is necessary to develop alternative immunotherapy approaches such as vaccines capable of stimulating a long-lasting antibody response as well as tumor-specific cytotoxic response.

Active immunotherapy strategies using DNA [10–12], peptide [13] or protein [14–16] vaccines against VEGF have been tested in preclinical studies. However, these strategies employed either harsh deliver systems or adjuvants not suitable for human use. It was shown that strong incomplete Freund's adjuvant (IFA) induced sequestration, dysfunction and deletion of tumor-specific $CD8^+$ T cells at vaccination sites in both mouse models [17] and human clinical trials [18], and therefore, cancer vaccines administered in IFA such as VEGF-kinoids [14] had limited efficacy of stimulating tumor-specific $CD8^+$ T cells.

In this study, we fused the receptor-binding domain of VEGF to diphtheria toxin T domain (DTT). The resulting protein DTT-VEGF was used to immunize mice. To our surprise, DTT-VEGF immunization not only stimulated strong neutralizing antibody response, but also induced type 1 immune response as well as anti-tumor cytotoxic T lymphocytes (CTLs) when coadministered with aluminum hydroxide (Alum) adjuvant. The vaccination reduced tumor vascular growth, enhanced $CD8^+$ T cell tumor infiltration and inhibited tumor growth.

Materials and methods

Mice and cell lines

Female C57BL/6 and BALB/c mice were purchased from Slaccas Laboratory Animal Inc. (Shanghai, China) and housed under pathogen-free conditions. Murine B16-F10 melanoma cell line and CT26 colon cancer cell line were purchased from the Cell Bank, Chinese Academy of Sciences (Shanghai, China) and were cultured in α-MEM and RPMI 1640 (Life Technologies, Carlsbad, CA, USA), respectively, supplemented with 10% FCS and 100 Units/ml penicillin and 100 μg/ml streptomycin (Life Technologies). All applicable international, national and/or institutional guidelines for the care and use of animals were followed.

Vector construction

The DNA fragments coding the amino acid residues 8–109 of human $VEGF_{165}$ [VEGF(8-109)] and 202–378 of diphtheria toxin were chemically synthesized with *Bam*H I and *Xho* I site at 5′ and 3′ ends, respectively. The DNA fragments were cloned in pGEX6p-1, respectively, to get expression plasmids pGEX-DTT and pGEX-VEGF. The DTT template was amplified by PCR using primers DTT-F and DTT-R (Supplementary Table 1). The VEGF template was amplified by PCR using primers VEGF-F and VEGF-R (Supplementary Table 1). The above templates were mixed and amplified by PCR using primers DTT-F and VEGF-R to produce the DTT-VEGF recombinant sequence. The PCR product was double-digested by *Bam*H I and *Xho* I and subsequently inserted in the plasmid pGEX6p-1 to generate expression plasmid pGEX-DTT-VEGF.

Protein expression, purification and structure modeling

The glutathione *S*-transferase (GST)-tagged proteins were expressed in *Escherichia coli* BL21 and purified by GST affinity chromatography (GE healthcare, Little Chalfont, UK). The GST tag was removed by PreScission Protease (GE healthcare) treatment. The proteins were stored at −70 °C in PBS until use.

The fusion protein DTT-VEGF was modeled using Ab Initio Domain Assembly Server (http://ffas.sanfordburnham.org/AIDA/) and visualized in Discovery Studio 3.0 (Accelrys, San Diego, CA).

DTT-VEGF adsorption by the Alum adjuvant and immunization

Alum (1.3% Alhydrogel) (Sigma-Aldrich, St. Louis, MO, USA) was serially diluted with PBS and mixed with equal volumes of DTT-VEGF (300 μg/ml) at room temperature for 30 min. Unadsorbed protein was quantified by measuring the absorbance at 280 nm of the supernatant after centrifugation of the antigen–adjuvant mixture at 12,000 rpm for 5 min. Adsorption rate was calculated using the following equation: adsorption rate = 1 − protein amount in the supernatant/total amount of input protein.

Mice were immunized three times subcutaneously at 2-week intervals with 200 μl of the vaccine formulation unless otherwise stated.

ELISA for antibody titer

Maxisorp 96-well plates (Thermo Scientific, Waltham, MA) were coated overnight at 4 °C with 100 μl of 0.1 μg/ml human $VEGF_{165}$ (Sino Biological Inc. Beijing, China) or 0.1 μg/ml mouse $VEGF_{164}$ (Sino Biological Inc.) in sodium carbonate buffer, pH 9.6. After washing and blocking, diluted mouse sera were added to wells and incubated for 1 h at room temperature. Bound antibodies were detected using 1:10,000 dilutions of goat anti-mouse Ig-specific subclass antibodies conjugated to HRP (Shanghai Immune Biotech Co. Ltd., Shanghai, China). Absorbance was determined at 450 nm using an EnSpire 2300 ELISA reader (PerkinElmer, Waltham, MA, USA). Antibody titers were represented as the reciprocal of the highest dilution with an absorbance of greater than 0.2 after subtracting the background.

Competitive ELISA for measurement of inhibition of the binding of VEGF to its receptor

Plates were coated overnight at 4 °C with 0.1 μg/ml human $VEGF_{165}$, followed by blocking with 3% skim milk. Diluted mouse sera were added and incubated for 1 h at room temperature. Then, 100 μl of 500 ng/ml human VEGFR2/FC (Sino Biological Inc.) was added and incubated for another 40 min. Wells were then washed and incubated with rabbit anti-human Fc IgG conjugated to HRP (Sino Biological Inc.). The bound antibody was detected as above antibody titer assay. Inhibition of VEGF/VEGFR2 interaction was calculated according to: inhibition = [1 − (A_{450} immune sera/A_{450nm} buffer control)] × 100%.

Lymphocyte proliferation assay

Mouse splenocytes were cultured in RPMI 1640 medium containing 10% FCS at a concentration of 1×10^5 cells/well, followed by stimulation with VEGF(8-109) protein (50 μg/ml) for 3 days. Con A (2 μg/ml) was used as positive control. Unstimulated splenocytes from immunized mice was set as negative control. Cell proliferation was measured using CCK-8 Kit (Beyotime Institute of Biotechnology, Nanjing, China). Stimulation index was defined as the ratio of $absorbance_{450nm}$ of stimulated cells to that of unstimulated cells.

In another set of experiments, splenocytes were first labeled with carboxyfluorescein succinimidyl ester (CFSE) (Molecular Probes, Eugene, OR, USA) and then cultured in RPMI 1640 medium containing 10% FCS, IL-2 (20 U/ml) and VEGF(8-109) (50 μg/ml). Anti-CD3/CD28-microbeads (Life Technologies) were used as positive control. Three days after culture, the cells were harvested and stained with anti-CD4-PE (GK1.5) (eBiosciences, San Diego, CA, USA) or anti-CD8-PE (53–6.7) (eBiosciences) Ab and analyzed by flow cytometry. Flow cytometry data were acquired by EpicsXL (Beckman Coulter, Brea, CA, USA), and data were analyzed using FlowJo software (Tree Star, Ashland, OR, USA). CD4- or CD8-positive cells were gated for generating the CFSE division profiles.

CTLs killing assay

Splenocytes were stimulated with VEGF(8-109) (50 μg/ml) for 3 days in the presence of 20 U/ml of recombinant human IL-2 (Peprotech, Rocky Hill, NJ, USA) and used as effector cells. VEGF-expressing B16-F10 cells [12] were used as target cells. Effector and target cells were mixed at various ratios in a final volume of 100 μl. After incubation for 4 h at 37 °C, 50 μl of the cultured media was collected to assess the amount of lactate dehydrogenase (LDH) using the CytoTox96 non-radioactive cytotoxicity assay kit (Promega, Madison, WI, USA).

Dendritic cells preparation

Bone marrow-derived DCs were obtained by culturing bone marrow cells of naïve C57BL/6 mice in culture medium containing GM-CSF (20 ng/ml) and IL-4 (20 ng/ml) (Peprotech) for 6 days as previously described [19]. DCs were pulsed with VEGF(8-109) (100 μg/ml) overnight and termed DC_{VEGF}.

Cytokines assay

Cytokines in mice sera were analyzed by a multiplex Luminex beads (Bio-Rad Laboratories, Hercules, CA, USA) according to the manufacturer's protocol, including the following cytokines: VEGF, type 1 (GM-CSF, IFN-γ, IL-2, IL-12p70 and TNF-α), type 2 (IL-4, IL-5 and IL-10).

For intracellular cytokine staining, $CD4^+$ or $CD8^+$ T cells were purified from the immunized mice by using negative selection kit (StemCell, Vancouver, BC, Canada)

and then cocultured with irradiated (4000 rads) DC_{VEGF} in the presence of GolgiStop (BD Biosciences, Mississauga, Ontario, Canada) for 6 h. Cells were then surface-stained with anti-CD4-FITC (GK1.5) (eBiosciences) or anti-CD8-FITC (53–6.7) (eBiosciences) Ab followed by intracellular staining with anti-IFN-γ-PE (XMG1.2) (eBiosciences), anti-IL-4-PE (11B11) (eBiosciences) or anti-IL-5-PE Ab (TRFK5) (eBiosciences) using Cytofix/Cytoperm Kit (BD Biosciences), and were analyzed by flow cytometry.

In vivo evaluation of anti-tumor effect

In the preventive vaccination setting, C57BL/6 mice were immunized three times subcutaneously at 2-week intervals. One week after the second immunization, the mice were injected subcutaneously into the right flank with 1×10^5 B16-F10 tumor cells or 3×10^5 CT26 tumor cells. In the therapeutic vaccination setting, mice were first challenged with 1×10^5 B16-F10 tumor cells, then immunized with 200 μl of the antigen–adjuvant preparation at the second day and boosted twice at weekly intervals. Days to tumor appearance, tumor volumes and survival were recorded. The length and width of tumors were measured three times a week with a caliper, and the volume of the tumors was calculated using the formula: tumor volume = (width^2 × length)/2. For ethical reason, mice bearing tumor with 2 cm in diameter were killed and recorded as dead. All animal experiments were repeated twice.

Immunohistochemistry

Tumors were fixed in 4% phosphate-buffered formalin for 24 h and then embedded in paraffin. The 5-μm sections were cut and stained with hematoxylin and eosin (H&E). Immunohistochemical detection of antigens in 5-μm paraffin sections was performed using the MaxVision TM kit (Fuzhou maixin Biological Inc., Fuzhou, China). The following primary antibodies were used: rabbit polyclonal to CD31 (ab28364, Abcam, Cambridge, UK), rat anti-mouse CD8α (53–6.7) (Santa Cruz Biotechnology Inc., Dallas, TX, USA). Microvessel areas were quantified using Image J (http://rsbweb.nih.gov/ij/) from five vessel hot-spot areas of each tumor section under 200× magnification. The percentages of $CD8^+$ cells were also quantified using Image J.

Statistical analysis

Student's *T* test or Mann–Whitney *U* test was used to compare the difference of two independent data. Cumulative survival time was calculated by the Kaplan–Meier method and analyzed by the Log-rank test. Probability values of $p < 0.05$ were considered statistically significant. Data are presented as mean ± standard error of mean (SEM).

Results

Design and expression of VEGF antigen

The VEGF gene has up to eight exons. Alternative exon splicing produces four major VEGF isoforms with the length of 121, 165, 189 and 206 amino acid residues, respectively. All four isoforms have an identical N-terminal domain (VEGF-110) [20]. The first seven residues, as well as the last residue of VEGF-110, are disordered in solution. VEGF(8-109) were crystallized and determined as the receptor-binding domain of VEGF [21]. Removal of the C-terminal domain of VEGF is associated with a significant loss in its bioactivity [22]. We hypothesized that immune response elicited by VEGF(8-109) may be capable of targeting all isoforms of VEGF and may have less risk of promoting tumor progression than intact VEGF does. To break the immune tolerance of VEGF, we selected DTT as an antigen carrier. The non-toxic mutant of diphtheria toxin CMR_{197} as a carrier protein has been used for many years and has an excellent safety record [23]. Interestingly, the DTT contains three universal T helper cell epitopes (residues 271–290, 321–350 and 351–370) that were recognized by $CD4^+$ T cells of more than 80% of human population [24]. To enhance the immune response to a particular epitope of an antigen, one rational strategy is to eliminate other potentially immunogenic domains that could 'dilute' the immune response. Therefore, we eliminated the N-terminal catalytic domain and C-terminal receptor-binding domain of diphtheria toxin, which contain multiple immunodominant B cell epitopes [25], and thus, only the T domain of diphtheria toxin was used as the antigen carrier. As DTT possesses a cysteine residue at the position of 201 of diphtheria toxin [26], we chose residues from 202 to 378 to avoid the formation of disulfide bonds between the DTT and VEGF which is a member of the cystine knot growth factor family. We fused VEGF(8-109) to the C terminus of DTT, named the resulting molecule as DTT-VEGF (Fig. 1a).

To improve the protein solvability, a hydrophilic Asp–Asp–Asp–Asp–Lys (DDDDK) sequence was fused to the N terminus of DTT-VEGF (Fig. 1b). DTT-VEGF and two control proteins, VEGF(8-109) and DTT, were expressed in *E. coli* as GST fusion proteins. After the removal of the GST tag, 2.5-mg DTT-VEGF was obtained from one liter of culture with purity of more than 95% (Fig. 1c). The gel filtration chromatography profile of the purified DTT-VEGF protein contained multiple peaks (Supplementary Figure 1a). Each peak fraction displayed a single band with same molecular weight on reducing SDS-PAGE (Supplementary Figure 1b). However, the fractions had different sizes on native-PAGE (Supplementary Figure 1c), indicating DTT-VEGF proteins are heterogeneous.

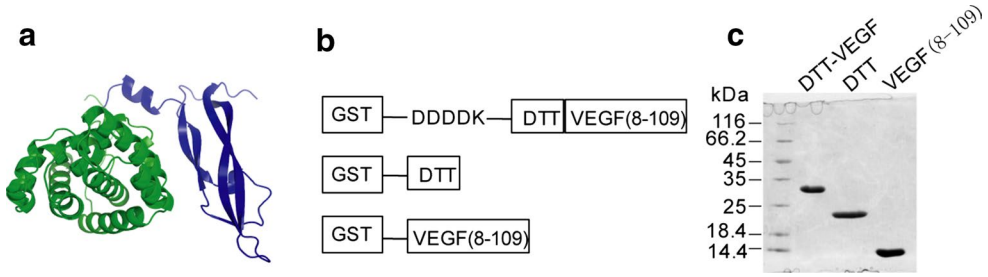

Fig. 1 Design and expression of VEGF-based antigen. **a** Structure model of DTT-VEGF. DTT domain is indicated in *green*. VEGF domain is shown in *blue*. **b** Schematic representation of GST-tagged DTT-VEGF, DTT and VEGF(8-109). **c** SDS-PAGE analysis of the purified recombinant proteins

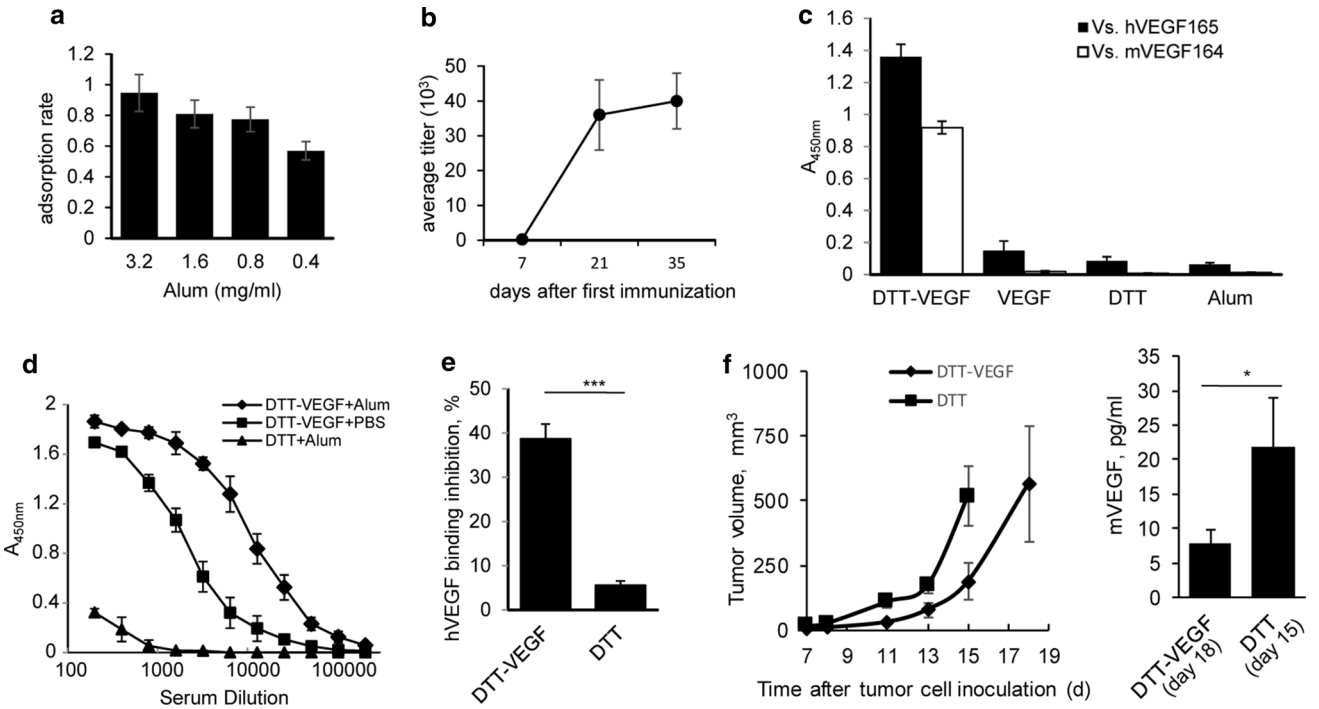

Fig. 2 DTT-VEGF immunization elicits neutralizing anti-VEGF antibody response. **a** The adsorption of DTT-VEGF to Alum adjuvant. The DTT-VEGF protein was mixed with different concentrations of Alum. The proteins adsorbed to Alum were determined by subtracting the proteins in the supernatant. **b**, **c** C57BL/6 mice ($n = 5$) were immunized three times with DTT-VEGF formulated with Alum at 2-week intervals. Sera were collected 1 week after each immunization. Anti-$hVEGF_{165}$ IgG titer kinetics was determined by ELISA (**b**). Sera collected 1 week after third immunization were diluted 100 times and tested for human $VEGF_{165}$ and mouse $VEGF_{164}$-specific IgG by ELISA (**c**). **d** C57BL/6 mice ($n = 5$) were immunized three times at 2-week intervals with DTT-VEGF formulated with Alum or PBS, respectively, Anti-$hVEGF_{165}$ IgG were determined at 1 week after third immunization. **e** C57BL/6 mice ($n = 5$) were immunized with DTT-VEGF or DTT, respectively, at 2-week intervals. Sera were collected 1 week after second immunization. $VEGF_{165}$ and $VEGR_2$ binding inhibition by sera (1:100 dilution) was assessed with competitive ELISA (**$p < 0.01$, Student's T test). **f** C57BL/6 mice ($n = 5$) were challenged subcutaneously with 1×10^5 B16-F10 tumor cells. One day later, the mice were immunized three times at weekly intervals. Tumor volumes were measured twice a week. Sera were collected when tumor volume reached 500 mm^3 (DTT-VEGF group on day 18, DTT group on 15, respectively, after tumor challenge), and the VEGF levels were determined by Luminex technology (*$p < 0.05$; Mann–Whitney U test). One representative experiment of two is shown

DTT-VEGF immunization elicits neutralizing antibody response

As the concentration of Alum can affect antigen adsorption and consequently the immunogenicity of the vaccine [27], the concentration of Alum was optimized. We found that 0.8 mg/ml of Alum efficiently adsorbed 80% of the antigen (Fig. 2a). Therefore, 0.8 mg/ml of Alum was used for this study. High titers of IgG to human $VEGF_{165}$ ($hVEGF_{165}$) were generated one week after the second immunization with DTT-VEGF + Alum (Fig. 2b). These IgGs also showed cross-reactivity to mouse $VEGF_{164}$ ($mVEGF_{164}$) (Fig. 2c). In contrast, VEGF(8-109) was not able to trigger antibody response (Fig. 2c), indicating that DTT helps

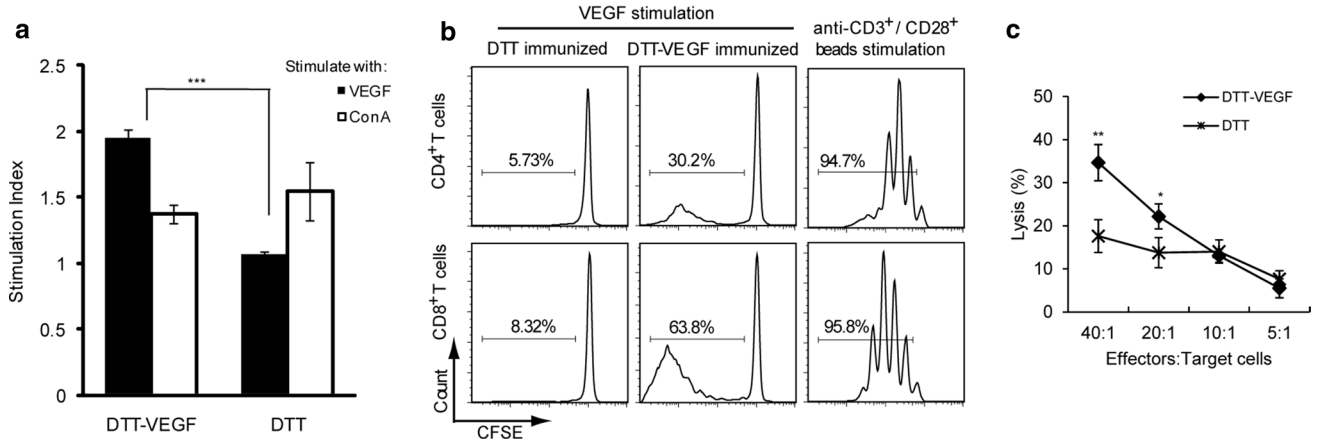

Fig. 3 DTT-VEGF immunization stimulates cellular immune response. C57BL/6 mice ($n = 3$) were immunized with DTT-VEGF or DTT, respectively, at 2-week intervals. **a** One week after the third immunization. Splenocytes were stimulated in vitro with VEGF(8-109) or ConA for 3 days. Cell proliferation was measured with CCK-8 method. **b** In vitro CFSE-labeled T cell proliferation assay. Splenocytes from immunized mice were labeled with CFSE and then stimulated with VEGF(8-109) (50 μg/ml). Anti-CD3/CD28 activation beads were used as positive control. Three days after culture, the cells were harvested and stained with anti-CD4-PE or anti-CD8-PE Ab and were analyzed by flow cytometry. CD4- or CD8-positive cells were gated for generating the CFSE division profiles. Percentages denote the fraction of cells that have undergone at least one division. **c** VEGF stimulated spleen cells from DTT-VEGF- or DTT-immunized mice were used as effector cells. VEGF-expressing B16-F10 tumor cells were used as target cells. In vitro cytotoxicity was assessed with LDH release method (**$p < 0.01$, *$p < 0.05$, Student's T test). One representative experiment of two is shown

to break immune self-tolerance. DTT-VEGF administered with Alum elicited much higher anti-VEGF antibody response than that with PBS (Fig. 2d).

VEGFR2 is the major signal transducer for VEGF-mediated angiogenesis [28]. We found that the binding of VEGF/VEGFR2 was inhibited by 40% using sera from DTT-VEGF-immunized mice (Fig. 2e), indicating that DTT-VEGF immunization elicited VEGF-specific neutralizing antibody response. In tumor-bearing mice, DTT-VEGF-vaccinated mice had lower serum VEGF compared with control mice (Fig. 2f), suggesting that tumor released VEGF was downregulated by circulating anti-VEGF neutralizing Abs in DTT-VEGF-immunized mice.

DTT-VEGF immunization stimulates cellular immune response

When the splenocytes from DTT-VEGF-immunized mice were stimulated with VEGF protein in vitro, a remarkable increase in cell proliferation was observed with stimulation index of ~2.0 in comparison with that of the control splenocytes (~1) (Fig. 3a). CFSE dilution profiles revealed that both $CD4^+$ T cell proliferation and $CD8^+$ T cell proliferation were stimulated by VEGF (Fig. 3b), indicating that DTT-VEGF immunization can generate a heightened T cell activation and memory.

To further confirm the activation of cellular immune response, the direct cytolytic activity of splenocytes of mice vaccinated with DTT-VEGF was analyzed 1 week after the third immunization using LDH release assay. The splenocytes from mice immunized with DTT-VEGF showed a significantly higher level of cytotoxic activity against B16-F10 cells expressing VEGF than those from the mice immunized with DTT (Fig. 3c).

DTT-VEGF immunization induces type 1 immunity

The antibody subclass analysis (Fig. 4a) showed that DTT-VEGF coadministered with Alum stimulated higher levels of IgG2a and IgG2b than that coadministered with PBS. High levels of IgM were only observed in mice immunized with DTT-VEGF in PBS. IgG1 level was slightly higher in Alum group, but it did not reach statistical significance. IgG3 was not induced in either formulation. These results demonstrated that Alum adjuvant not only enhanced the antibody response of DTT-VEGF, but also promoted the antibody maturation from IgM to IgG subclass. Of note, the ratios of Ig2a/IgG1 and Ig2b/IgG1 for mice immunized with DTT-VEGF formulated with Alum were greater than 1, while these ratios were less than 1 for mice immunized with DTT-VEGF in PBS, suggesting that formulation of DTT-VEGF with Alum enhanced type 1 immunity. We further performed flow cytometric analyses to measure intracellular cytokine expression. $CD4^+$ T cells (0.6%) (Fig. 4b), as well as 0.4% of $CD8^+$ T cells (Fig. 4c), from DTT-VEGF-immunized mice expressed IFN-γ after stimulation with DC_{VEGF}. However, neither IL-4-producing (Fig. 4b, c) nor IL-5-producing (data not shown) T cells

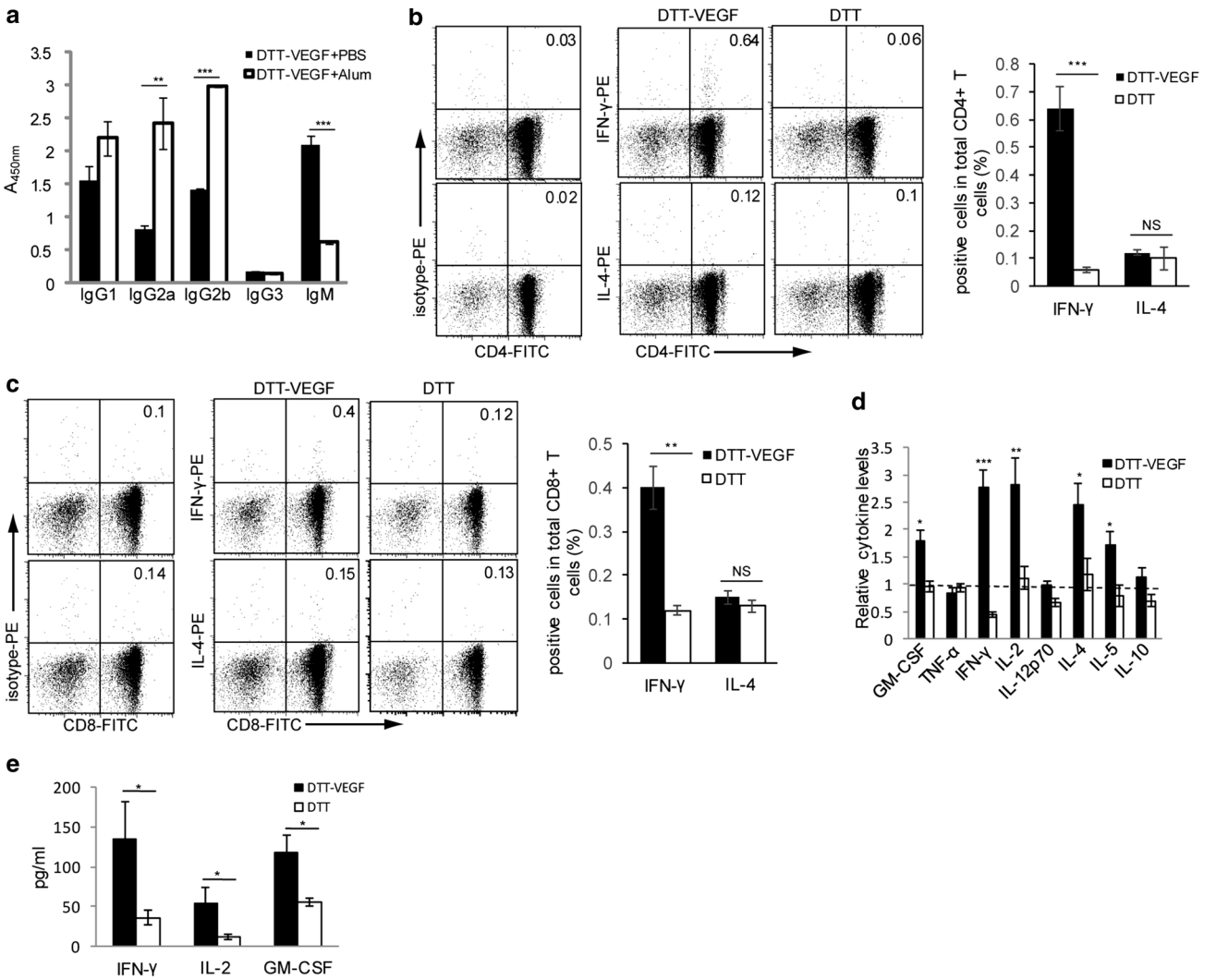

Fig. 4 DTT-VEGF immunization induces type 1 immune response. **a** C57BL/6 mice ($n = 5$) were immunized with DTT-VEGF formulated with Alum or PBS three times at 2-week intervals, and sera were collected one week after the last immunization. Ig subclass was determined by ELISA. $***p < 0.001$; $**p < 0.01$, Student's T test. **b**, **c** C57BL/6 mice ($n = 3$) were immunized with DTT-VEGF or DTT, respectively, at 2-week intervals. One week after the third immunization. $CD4^+$ (**b**) or $CD8^+$ (**c**) T cells were purified from the immunized mice and then were cocultured with irradiated DC_{VEGF} in the presence of GolgiStop; 6 h later, the cells were harvested and stained with anti-CD4-FITC or anti-CD8-FITC Ab. After permeabilization, the cells were stained for intracellular cytokine and analyzed by flow cytometry. The *value in each panel* represents the percentage of cytokine-producing cells in the total $CD4^+$ or $CD8^+$ T cell population. $***p < 0.001$, $**p < 0.01$. Student's T test. **d**, **e** C57BL/6 mice ($n = 5$) were immunized with DTT-VEGF or DTT, respectively, at 2-week intervals. One week after the third immunization, the mice were challenged with 1×10^5 B16-F10 tumor cells. Sera were collected 1 d before and 14 d after tumor challenge, and the cytokines levels were quantified using Luminex technology. The relative cytokine levels before tumor challenge were defined as the fold change compared to the unimmunized mice (**d**). The type 1 cytokine levels in the sera after tumor challenge are shown in **e**. $*p < 0.05$, Mann–Whitney U test. One representative experiment of two is shown

specific to VEGF were detectable, suggesting a type 1 bias response to this vaccine. DTT-VEGF immunization significantly promoted the production of type 1 cytokines such as GM-CSF, IFN-γ and IL-2 (Fig. 4d). After tumor challenge, significantly higher levels of IFN-γ, IL-2 and GM-CSF were observed in DTT-VEGF-immunized mice compared to DTT-immunized mice (Fig. 4e).

No adverse tissue damage following DTT-VEGF immunization

DTT-VEGF-immunized mice survived with normal growth, and the wound of tail healed normally after blood collection (data not shown), suggesting the lack of adverse effects associated with circulating anti-VEGF neutralizing

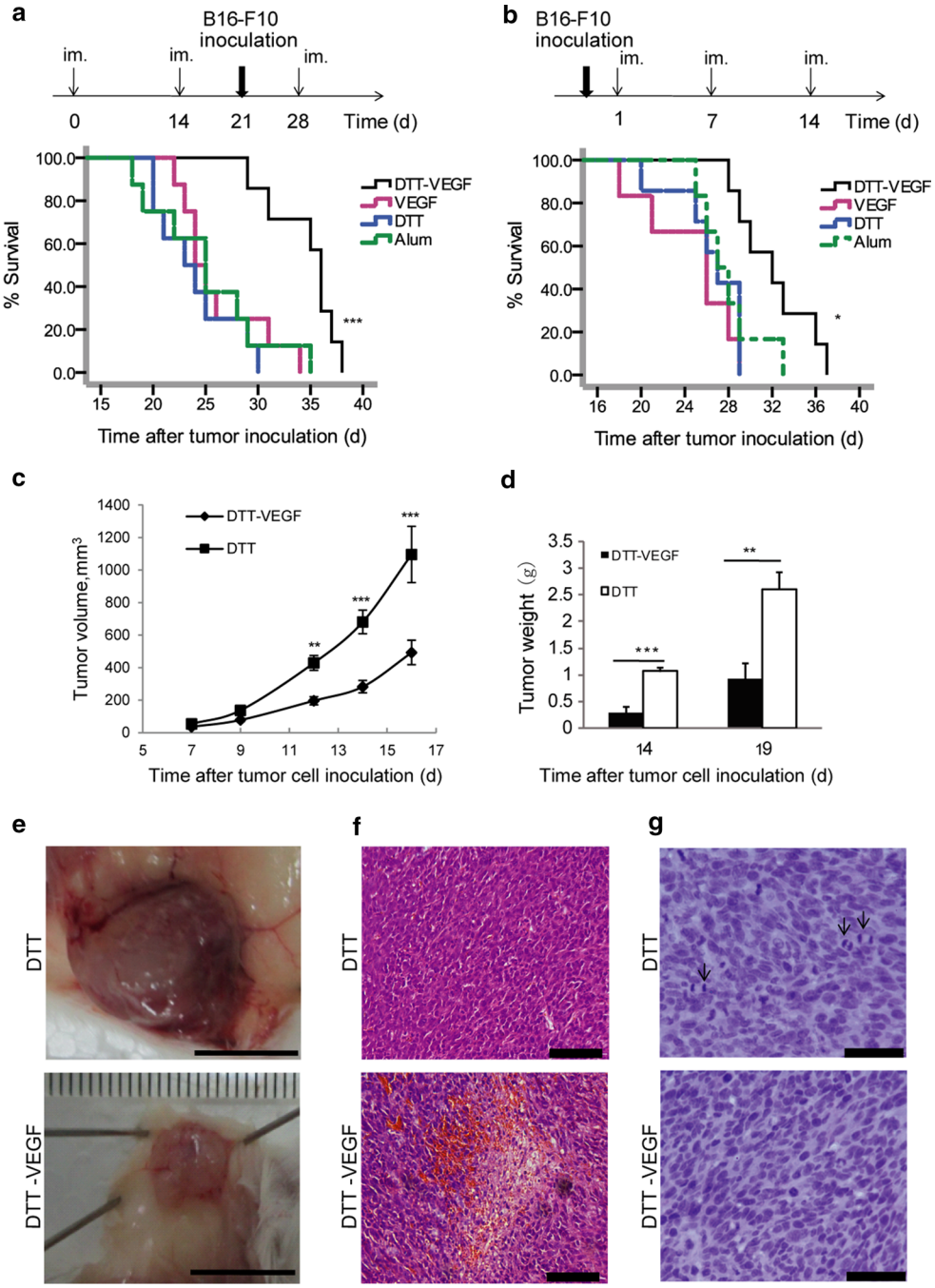

Fig. 5 DTT-VEGF vaccine inhibits tumor growth. **a** Survival rates of mice after the tumor challenge in preventive vaccination. C57BL/6 mice ($n = 8$) were immunized (im.) three times at 2-week intervals. One week after the second immunization, the mice were challenged subcutaneously with 1×10^5 B16-F10 tumor cells. ***$p < 0.001$, Log-rank test. **b** Survival rates of mice after the tumor challenge in therapeutic vaccination. C57BL/6 mice ($n = 8$) were challenged subcutaneously with 1×10^5 B16-F10 tumor cells. One day later, the mice were immunized three times at weekly intervals. *$p < 0.05$, Log-rank test. **c**–**g** BALB/c mice ($n = 10$) were vaccinated with three immunization of DTT-VEGF or DTT at 2-week intervals. Immunized mice were challenged subcutaneously with 3×10^5 CT26 tumor cells 1 week after the second immunization. Tumors volumes were measured at indicated times (**c**). Tumors were excised and weighted (**d**). ***$p < 0.001$, **$p < 0.01$, Mann–Whitney *U* test. Macroscopic appearance of CT26 tumors (**e**). *Scar bar* 1 cm. H&E staining of CT26 tumor sections shows necrosis in tumors from DTT-VEGF-immunized mice (**f**). *Scar bar* 100 μm. Hematoxylin staining shows mitosis (indicated by *arrows*) in tumors from DTT-immunized mice (**g**). *Scar bar* 50 μm. Data are representative of three independent experiments

Abs. Moreover, H&E staining of liver, spleen and kidney sections did not show any differences between the non-immunized and the DTT-VEGF-immunized mice (Supplementary Figure 2a–c), indicating that DTT-VEGF immunization is safe.

DTT-VEGF vaccination inhibits tumor growth

In preventive vaccination, the survival of B16-F10 tumor-bearing mice was significantly prolonged in the DTT-VEGF-immunized group when compared to three control groups (Fig. 5a). The mean survival time increased from less than 25 days in the control groups to 35 days in the DTT-VEGF group. In the therapeutic vaccination, a significantly prolonged survival was also observed in the mice immunized with DTT-VEGF (Fig. 5b). The mean survival time of the DTT-VEGF group was 32 days, while that of the control groups were 25 days.

Murine colorectal CT26 tumor which expresses much lower level of VEGF compared to B16-F10 cells [4, 12] was used to confirm the anti-tumor effect of the DTT-VEGF vaccination. Immunization with DTT-VEGF

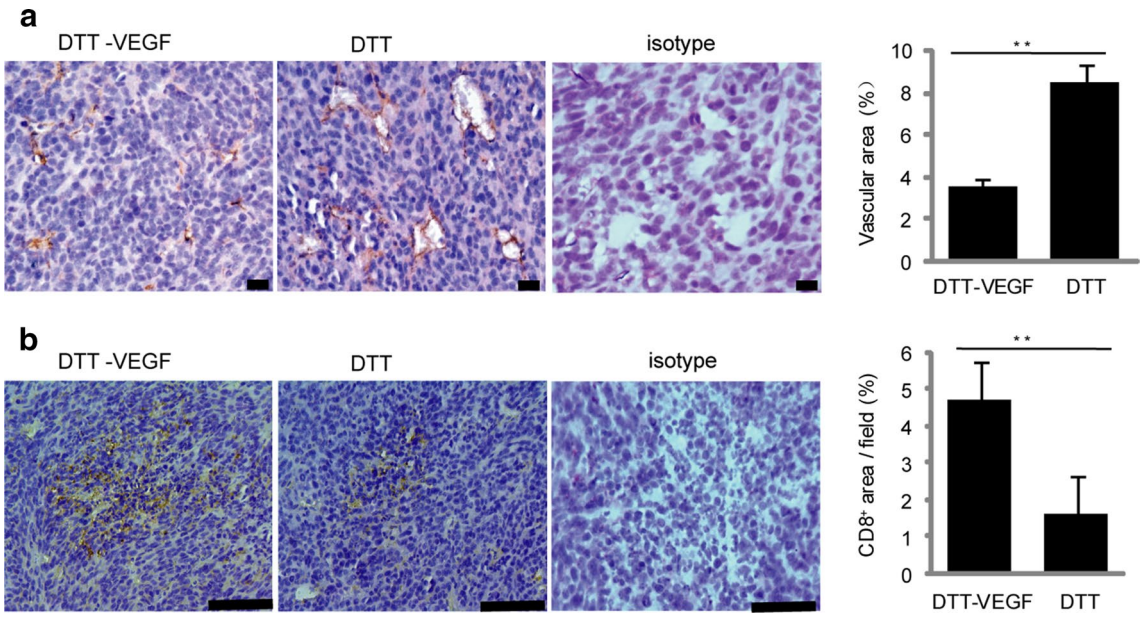

Fig. 6 DTT-VEGF vaccine reduces tumor vascular growth and enhances T cell infiltration. CT26 tumors ($n = 5$) were collected at day 14 after tumor challenge as in Fig. 5d, sectioned and immunohistochemically stained. **a** Immunohistochemical staining of $CD31^+$ cells. *Scale bar* 20 μm. Quantification of $CD31^+$ blood vessels (mean % of CD31-covered area/field ± SEM) is shown in the *bar graph on the right*. **b** Immunohistochemical staining of $CD8^+$ cells. *Scale bar* 100 μm. Quantification of $CD8^+$ cells (mean % of $CD8^+$-covered area/field ± SEM) is represented in the *bar graph on the right*. $^{**}p < 0.01$, Mann–Whitney *U* test

resulted in significant inhibition of growth (Fig. 5c). Tumor weights of DTT-VEGF-immunized mice were much less than that of DTT-immunized mice (Fig. 5d). Moreover, tumors from DTT-treated mice were surrounded by large and branched blood vessels, which were not seen in DTT-VEGF-immunized mice (Fig. 5e). Furthermore, tumor sections from DTT-VEGF-immunized mice showed extensive necrosis and hemorrhage, which were not seen in tumor sections from DTT-treated mice (Fig. 5f). In contrast, extensive mitosis was observed in tumors from DTT-treated mice (Fig. 5g). To rule out the possibility that the differences of tumor micromorphology are due to differences in tumor size, tumors were collected when the diameters reached 1 cm for H&E staining. The above differences of tumor micromorphology were also observed between the DTT-VEGF-immunized mice and DTT-treated mice (Supplementary Figure 3a–b).

DTT-VEGF vaccination reduces tumor vascular growth and enhances T cell infiltration

To investigate how the anti-VEGF immune response affects the tumor vasculature, the $CD31^+$ tumor blood vessels were analyzed by immunostaining. Small vessels without lumen were seen in the tumor from DTT-VEGF-immunized mice, while disorganized vessels with large lumen formed in the tumor from the DTT-immunized mice (Fig. 6a). Furthermore, the $CD31^+$-positive vascular areas in the tumor sections from DTT-VEGF-immunized mice were significantly less than that from DTT-treated mice (Fig. 6a). VEGF has been shown to suppress the expression of adhesion molecules in tumor vascular endothelium involved in leukocyte trafficking [5], and thus, counteracting VEGF may make tumors more vulnerable to immune system. To evaluate whether the anti-VEGF immune response could promote immune cells infiltration to tumor tissue, we analyzed the amount of $CD8^+$ T cells in the tumors from DTT-VEGF-and DTT-vaccinated mice, respectively. The number of $CD8^+$-positive cells in the tumor from DTT-VEGF-immunized mice was significantly higher than that from DTT-treated mice (Fig. 6b). These results suggest that the decrease of tumor volume was at least in part caused by reduced tumor vasculature and increased T cell infiltration.

Discussion

Cancer vaccines targeting a single protein mutated or overexpressed in cancer cells have been of limited success in clinic trials [29]. This is partly due to the fact that tumor tissues have extensive heterogeneity at genetic and epigenetic levels [30], and vaccines targeting single tumor-associated antigen can only achieve short-term tumor shrinkage, but little benefit on the overall survival rates [31]. Moreover, it is still time- and labor-consuming to identify the mutation suitable for developing promising cancer

vaccine. For example, by combining mass spectrometry and exome sequencing, >1300 amino acid changes were identified; however, only three mutations were validated as immunogenic neo-antigens [32]. Targeting the tumor vasculature with vaccines may be more effective than targeting tumor cells due to the genetic stability of endothelial cells and the amplifying inhibit effect thereof [33]. VEGF-mediated signaling is the key step in tumor vasculature formation. VEGF-based gene therapy [10–12] and endothelial cell-based vaccines [34] have been tested to inhibit tumor angiogenesis. However, protein vaccines have potential advantages with respect to antigen specificity, manufacturing feasibility and safety. In this study, we show that a rationally designed VEGF protein vaccine is highly immunogenic and can induce strong anti-tumor immunity in mouse models.

Rational antigen design is crucial to the development of protein vaccine. A potential limitation for some protein vaccines is the lack of sufficient T cell epitopes to help the antibody responses. Our data demonstrate that the universal T helper epitopes in DTT are helpful for the VEGF antibody affinity maturation. Increasing evidences showed that the VEGF level was associated with tumor progression and aggressiveness [35], and thus, treating cancer patients with intact VEGF could encounter safety issues when applying for human vaccine clinical trials. The receptor-binding domain VEGF(8-109) is a safer vaccine than intact VEGF as it lacks mitogenic potencies to endothelial cell [22]. Considering that strong adjuvants such as IFA may induce sequestration, dysfunction and deletion of tumor-specific $CD8^+$ T cells at vaccination sites [17, 18] and that strong adjuvants may lead to severe adverse reactions when used in human trails, Alum, which has been approved for use in humans and has vast health implications [36], was used as adjuvant in the our VEGF vaccine formulation. Hopefully, there might be few obstacles for the translation of this approach into clinical applications.

Type 1 response is characterized by enhanced secretion of IFN-γ, TNF-α and IL-12, and the induction of IgG2a and CTLs, while type 2 response is characterized by the secretion of IL-4 and IL-5 [37]. It is generally considered that type 1 response inhibits tumor growth, while type 2 promotes tumor growth [38]. Patients with metastatic melanoma exist in a state of systemic type 2 dominant immune homeostasis that could be at least in part mediated by tumor-derived VEGF [39]. Profound tumor-specific type 2 bias was also found in patients with malignant glioma [40]. Hence, combining VEGF-targeting therapy with vaccine strategies to skew tumor antigen-specific T cell response toward type 1 bias may provide more survival advantage. Alum adjuvant is in limited use in cancer vaccines due to their tendency to skew the immune response toward a type 2 response [36]. However, it was recently shown that injection of Alum alone into mice carrying H22 hepatocarcinoma triggered anti-tumor $CD8^+$ T cell response [41]. We showed that DTT-VEGF administered with Alum induced type 1 response characterized by the induction of VEGF-specific IgG2a and IgG2b antibodies, type 1 cytokines and tumor-specific cytotoxic response, highlighting its potential as an effective vaccine for human cancers. Since we observed the increase of type 1 cytokines in DTT-VEGF-immunized mice, but not in the DTT-immunized mice, it can be inferred that the immune response elicited by VEGF might promote type 1 cytokine production. This result is consistent with previous report that blocking VEGF with bevacizumab combined with chemotherapy promotes type 1 inflammatory response [42].

Tumor-infiltrating $CD8^+$ T cells have a positive association with prognosis in cancer patients [43, 44]. One challenge for developing therapeutic cancer vaccine is to improve the effective trafficking of cancer-specific T cells to the tumor sites. Considerable work to unravel mechanisms for T cell trafficking has revealed that pro-angiogenic factors such as VEGF were able to downregulate intercellular adhesion molecule 1 on the surface of endothelial cells and subsequently suppress leukocyte infiltration [5]. It is therefore reasonable to hypothesize that inhibition of VEGF signaling pathway may circumvent this problem. It has been shown that lower doses of an anti-VEGFR2 antibody resulted in vascular normalization and facilitated $CD4^+$ and $CD8^+$ T cell tumor infiltration [45]. Consistently, we found that DTT-VEGF immunization reduced tumor angiogenesis and enhanced $CD8^+$ T cell infiltration.

It remains elusive how the type 1 immune response and VEGF-specific CTLs are stimulated with the Alum-formulated DTT-VEGF vaccine. It is possible that DTT-VEGF antigen may be delivered into the DCs via endocytic uptake with the help of Alum adjuvant [46]. The properties of membrane insertion and translocation of DTT [47] in the low pH environment of endosome may facilitate the delivering of VEGF epitopes to MHC class I pathway, thereby stimulating cytotoxic activity. However, clarification of these details needs further analyses. If it is confirmed, this study may show a general vaccine strategy of targeting other cancer antigens.

In conclusion, DTT-VEGF fusion protein administered with Alum adjuvant inhibits tumor growth by promoting type 1 immune response and $CD8^+$ T cell infiltration in addition to anti-angiogenesis, indicating its potential as a promising cancer vaccine.

Acknowledgements This work was supported by National S and T major projects of China (Key Innovative Drug Development) (No. 2014ZX09101043), Shanghai Municipal Science and Technology Program (No. 14431904100), Shanghai Industry-Academia-Research Collaboration Program (No. CXY-2013-54), Medicine Science/Engineering Hybrid Project of Shanghai Jiao Tong University (No.

YG2013MS09) and Specialized Research Fund for the Doctoral Program of Higher Education of China (SRFDP) (No. 20130073120110).

Compliance with ethical standards

Conflict of interest The authors declare that they have no conflict of interest.

References

1. Ferrara N, Kerbel RS (2005) Angiogenesis as a therapeutic target. Nature 438:967–974. doi:10.1038/Nature04483
2. Mimura K, Kono K, Takahashi A, Kawaguchi Y, Fujii H (2007) Vascular endothelial growth factor inhibits the function of human mature dendritic cells mediated by VEGF receptor-2. Cancer Immunol Immunother 56:761–770. doi:10.1007/s00262-006-0234-7
3. Ohm JE, Gabrilovich DI, Sempowski GD, Kisseleva E, Parman KS, Nadaf S, Carbone DP (2003) VEGF inhibits T-cell development and may contribute to tumor-induced immune suppression. Blood 101:4878–4886. doi:10.1182/blood-2002-07-1956
4. Terme M, Pernot S, Marcheteau E, Sandoval F, Benhamouda N, Colussi O, Dubreuil O, Carpentier AF, Tartour E, Taieb J (2013) VEGFA-VEGFR pathway blockade inhibits tumor-induced regulatory T-cell proliferation in colorectal cancer. Cancer Res 73:539–549. doi:10.1158/0008-5472.CAN-12-2325
5. Griffioen AW (2008) Anti-angiogenesis: making the tumor vulnerable to the immune system. Cancer Immunol Immunother 57:1553–1558. doi:10.1007/s00262-008-0524-3
6. Miller K, Wang M, Gralow J, Dickler M, Cobleigh M, Perez EA, Shenkier T, Cella D, Davidson NE (2007) Paclitaxel plus bevacizumab versus paclitaxel alone for metastatic breast cancer. N Engl J Med 357:2666–2676. doi:10.1056/NEJMoa072113
7. Sandler A, Gray R, Perry MC, Brahmer J, Schiller JH, Dowlati A, Lilenbaum R, Johnson DH (2006) Paclitaxel-carboplatin alone or with bevacizumab for non-small-cell lung cancer. N Engl J Med 355:2542–2550. doi:10.1056/NEJMoa061884
8. Hurwitz H, Fehrenbacher L, Novotny W, Cartwright T, Hainsworth J, Heim W, Berlin J, Baron A, Griffing S, Holmgren E, Ferrara N, Fyfe G, Rogers B, Ross R, Kabbinavar F (2004) Bevacizumab plus irinotecan, fluorouracil, and leucovorin for metastatic colorectal cancer. N Engl J Med 350:2335–2342. doi:10.1056/NEJMoa032691
9. Ebos JM, Kerbel RS (2011) Antiangiogenic therapy: impact on invasion, disease progression, and metastasis. Nat Rev Clin Oncol 8:210–221. doi:10.1038/nrclinonc.2011.21
10. Wei YQ, Huang MJ, Yang L, Zhao X, Tian L, Lu Y, Shu JM, Lu CJ, Niu T, Kang B, Mao YQ, Liu F, Wen YJ, Lei S, Luo F, Zhou LQ, Peng F, Jiang Y, Liu JY, Zhou H, Wang QR, He QM, Xiao F, Lou YY, Xie XJ, Li Q, Wu Y, Ding ZY, Hu B, Hu M, Zhang W (2001) Immunogene therapy of tumors with vaccine based on Xenopus homologous vascular endothelial growth factor as a model antigen. Proc Natl Acad Sci USA 98:11545–11550
11. Kyutoku M, Nakagami H, Koriyama H, Tomioka H, Nakagami F, Shimamura M, Kurinami H, Zhengda P, Jo DH, Kim JH, Takakura N, Morishita R (2013) Development of novel DNA vaccine for VEGF in murine cancer model. Sci Rep 3:3380. doi:10.1038/srep03380
12. Bequet-Romero M, Ayala M, Acevedo BE, Rodriguez EG, Ocejo OL, Torrens I, Gavilondo JV (2007) Prophylactic naked DNA vaccination with the human vascular endothelial growth factor induces an anti-tumor response in C57Bl/6 mice. Angiogenesis 10:23–34. doi:10.1007/s10456-006-9062-9
13. Wang B, Kaumaya PTP, Cohn DE (2010) Immunization with synthetic VEGF peptides in ovarian cancer. Gynecol Oncol 119:564–570. doi:10.1016/j.ygyno.2010.07.037
14. Rad FH, Le Buanec H, Paturance S, Larcier P, Genne P, Ryffel B, Bensussan A, Bizzini B, Gallo RC, Zagury D, Uzan G (2007) VEGF kinoid vaccine, a therapeutic approach against tumor angiogenesis and metastases. Proc Natl Acad Sci USA 104:2837–2842. doi:10.1073/pnas.0611022104
15. Morera Y, Bequet-Romero M, Ayala M, Lamdan H, Agger EM, Andersen P, Gavilondo JV (2008) Anti-tumoral effect of active immunotherapy in C57BL/6 mice using a recombinant human VEGF protein as antigen and three chemically unrelated adjuvants. Angiogenesis 11:381–393. doi:10.1007/s10456-008-9121-5
16. Kamstock D, Elmslie R, Thamm D, Dow S (2007) Evaluation of a xenogeneic VEGF vaccine in dogs with soft tissue sarcoma. Cancer Immunol Immunother 56:1299–1309. doi:10.1007/s00262-007-0282-7
17. Hailemichael Y, Dai Z, Jaffarzad N, Ye Y, Medina MA, Huang XF, Dorta-Estremera SM, Greeley NR, Nitti G, Peng W, Liu C, Lou Y, Wang Z, Ma W, Rabinovich B, Schluns KS, Davis RE, Hwu P, Overwijk WW (2013) Persistent antigen at vaccination sites induces tumor-specific CD8(+) T cell sequestration, dysfunction and deletion. Nat Med 19:465–472. doi:10.1038/nm.3105
18. Salerno EP, Shea SM, Olson WC, Petroni GR, Smolkin ME, McSkimming C, Chianese-Bullock KA, Slingluff CL Jr (2013) Activation, dysfunction and retention of T cells in vaccine sites after injection of incomplete Freund's adjuvant, with or without peptide. Cancer Immunol Immunother 62:1149–1159. doi:10.1007/s00262-013-1435-5
19. Chen Z, Dehm S, Bonham K, Kamencic H, Juurlink B, Zhang X, Gordon JR, Xiang J (2001) DNA array and biological characterization of the impact of the maturation status of mouse dendritic cells on their phenotype and antitumor vaccination efficacy. Cell Immunol 214:60–71
20. Harper SJ, Bates DO (2008) VEGF-A splicing: the key to anti-angiogenic therapeutics? Nat Rev Cancer 8:880–887. doi:10.1038/nrc2505
21. Christinger HW, Muller YA, Berleau LT, Keyt BA, Cunningham BC, Ferrara N, de Vos AM (1996) Crystallization of the receptor binding domain of vascular endothelial growth factor. Proteins 26:353–357. doi:10.1002/(SICI)1097-0134(199611)26:3<353:AID-PROT9>3.0.CO;2-E
22. Keyt BA, Berleau LT, Nguyen HV, Chen H, Heinsohn H, Vandlen R, Ferrara N (1996) The carboxyl-terminal domain (111-165) of vascular endothelial growth factor is critical for its mitogenic potency. J Biol Chem 271:7788–7795
23. Shinefield HR (2010) Overview of the development and current use of CRM(197) conjugate vaccines for pediatric use. Vaccine 28:4335–4339. doi:10.1016/j.vaccine.2010.04.072
24. Diethelm-Okita BM, Okita DK, Banaszak L, Conti-Fine BM (2000) Universal epitopes for human $CD4^+$ cells on tetanus and diphtheria toxins. J Infect Dis 181:1001–1009. doi:10.1086/315324
25. Romaniuk SI, Kolybo DV, Komisarenko SV (2012) Recombinant diphtheria toxin derivatives: perspectives of application. Russ J Bioorg Chem 38:565–577. doi:10.1134/s106816201206012x
26. Choe S, Bennett MJ, Fujii G, Curmi PM, Kantardjieff KA, Collier RJ, Eisenberg D (1992) The crystal structure of diphtheria toxin. Nature 357:216–222. doi:10.1038/357216a0
27. Hansen B, Sokolovska A, HogenEsch H, Hem SL (2007) Relationship between the strength of antigen adsorption to an aluminum-containing adjuvant and the immune response. Vaccine 25:6618–6624. doi:10.1016/j.vaccine.2007.06.049
28. Shibuya M (2011) Vascular endothelial growth factor (VEGF) and its receptor (VEGFR) signaling in angiogenesis: a crucial

target for anti- and pro-angiogenic therapies. Genes Cancer 2:1097–1105. doi:10.1177/1947601911423031
29. Melero I, Gaudernack G, Gerritsen W, Huber C, Parmiani G, Scholl S, Thatcher N, Wagstaff J, Zielinski C, Faulkner I, Mellstedt H (2014) Therapeutic vaccines for cancer: an overview of clinical trials. Nat Rev Clin Oncol 11:509–524. doi:10.1038/nrclinonc.2014.111
30. McGranahan N, Swanton C (2015) Biological and therapeutic impact of intratumor heterogeneity in cancer evolution. Cancer Cell 27:15–26. doi:10.1016/j.ccell.2014.12.001
31. Schlom J (2012) Therapeutic cancer vaccines: current status and moving forward. J Natl Cancer Inst 104:599–613. doi:10.1093/jnci/djs033
32. Yadav M, Jhunjhunwala S, Phung QT, Lupardus P, Tanguay J, Bumbaca S, Franci C, Cheung TK, Fritsche J, Weinschenk T, Modrusan Z, Mellman I, Lill JR, Delamarre L (2014) Predicting immunogenic tumour mutations by combining mass spectrometry and exome sequencing. Nature 515:572–576. doi:10.1038/nature14001
33. Matejuk A, Leng Q, Chou ST, Mixson AJ (2011) Vaccines targeting the neovasculature of tumors. Vasc Cell 3:7. doi:10.1186/2045-824X-3-7
34. Chen XY, Zhang W, Wu S, Bi F, Su YJ, Tan XY, Liu JN, Zhang J (2006) Vaccination with viable human umbilical vein endothelial cells prevents metastatic tumors by attack on tumor vasculature with both cellular and humoral immunity. Clin Cancer Res 12:5834–5840. doi:10.1158/1078-0432.CCR-06-1105
35. Poon RT, Fan ST, Wong J (2001) Clinical implications of circulating angiogenic factors in cancer patients. J Clin Oncol 19:1207–1225
36. Hogenesch H (2012) Mechanism of immunopotentiation and safety of aluminum adjuvants. Front Immunol 3:406. doi:10.3389/fimmu.2012.00406
37. Spellberg B, Edwards JE Jr (2001) Type 1/Type 2 immunity in infectious diseases. Clin Infect Dis 32:76–102. doi:10.1086/317537
38. Grivennikov SI, Greten FR, Karin M (2010) Immunity, inflammation, and cancer. Cell 140:883–899. doi:10.1016/j.cell.2010.01.025
39. Nevala WK, Vachon CM, Leontovich AA, Scott CG, Thompson MA, Markovic SN (2009) Evidence of systemic Th2-driven chronic inflammation in patients with metastatic melanoma. Clin Cancer Res 15:1931–1939. doi:10.1158/1078-0432.CCR-08-1980
40. Shimato S, Maier LM, Maier R, Bruce JN, Anderson RC, Anderson DE (2012) Profound tumor-specific Th2 bias in patients with malignant glioma. BMC Cancer 12:561. doi:10.1186/1471-2407-12-561
41. Wang B, Wang X, Wen Y, Fu J, Wang H, Ma Z, Shi Y (2015) Suppression of established hepatocarcinoma in adjuvant only immunotherapy: alum triggers anti-tumor CD8(+) T cell response. Sci Rep 5:17695. doi:10.1038/srep17695
42. Tsavaris N, Voutsas IF, Kosmas C, Gritzapis AD, Baxevanis CN (2012) Combined treatment with bevacizumab and standard chemotherapy restores abnormal immune parameters in advanced colorectal cancer patients. Invest New Drugs 30:395–402. doi:10.1007/s10637-010-9533-0
43. Erdag G, Schaefer JT, Smolkin ME, Deacon DH, Shea SM, Dengel LT, Patterson JW, Slingluff CL Jr (2012) Immunotype and immunohistologic characteristics of tumor-infiltrating immune cells are associated with clinical outcome in metastatic melanoma. Cancer Res 72:1070–1080. doi:10.1158/0008-5472.CAN-11-3218
44. Noble F, Mellows T, McCormick Matthews LH, Bateman AC, Harris S, Underwood TJ, Byrne JP, Bailey IS, Sharland DM, Kelly JJ, Primrose JN, Sahota SS, Bateman AR, Thomas GJ, Ottensmeier CH (2016) Tumour infiltrating lymphocytes correlate with improved survival in patients with oesophageal adenocarcinoma. Cancer Immunol Immunother 65:651–662. doi:10.1007/s00262-016-1826-5
45. Huang Y, Yuan J, Righi E, Kamoun WS, Ancukiewicz M, Nezivar J, Santosuosso M, Martin JD, Martin MR, Vianello F, Leblanc P, Munn LL, Huang P, Duda DG, Fukumura D, Jain RK, Poznansky MC (2012) Vascular normalizing doses of antiangiogenic treatment reprogram the immunosuppressive tumor microenvironment and enhance immunotherapy. Proc Natl Acad Sci USA 109:17561–17566. doi:10.1073/pnas.1215397109
46. Flach TL, Ng G, Hari A, Desrosiers MD, Zhang P, Ward SM, Seamone ME, Vilaysane A, Mucsi AD, Fong Y, Prenner E, Ling CC, Tschopp J, Muruve DA, Amrein MW, Shi Y (2011) Alum interaction with dendritic cell membrane lipids is essential for its adjuvanticity. Nat Med 17:479–487. doi:10.1038/nm.2306
47. Kyrychenko A, Posokhov YO, Rodnin MV, Ladokhin AS (2009) Kinetic intermediate reveals staggered pH-dependent transitions along the membrane insertion pathway of the diphtheria toxin T-domain. Biochemistry 48:7584–7594. doi:10.1021/bi9009264